Mathematical modelling of mobile bed filtration with contact flocculation — filtration arrangement

S Vigneswaran and C Visvanathan

In conventional water treatment plants, the unit operations such as rapid mixing, flocculation, sedimentation, filtration and disinfection are used. All these pretreatment units lead to an increase in operational and capital costs. In some cases depending on the raw water characteristics, few of these unit operations can be eliminated. Direct filtration is one of the recent developments in the filtration processes. This filtration system is being designed with only screening, coagulant addition, rapid-mixing and flocculation prior to filtration. Contact flocculation-filtration is a further modification of direct filtration, with only chemical holding tank in the pretreatment unit. Therefore, large capital and operational cost savings can be achieved by this process (Figure 1) if it is technically feasible for the raw water to be treated. The main drawback of this treatment method is the frequent clogging of the filter bed, since the total removal of the suspended matter occurs within the filter bed. Therefore, the filter bed requires frequent backwashing. This frequent filter bed clogging problem during contact flocculation-filtration has led to the development of mobile bed filters. This type of filter arrangement is designed such that the filter grains at the bottom layer are recycled to the top of the filter bed using an air-lift system. Here the recycled filter grains are washed continuously. This process eliminates the problem of backwashing and functions as a continuous filter. There exists several types of design for mobile bed filtration.[1,2,3,4]

Mathematical formulation of suspended solids removal in contact-flocculation filtration is complex since both flocculation and suspended solids removal occur within the filter bed itself. In this study, a mathematical formulation based on O'Melia and Alis' model[5] was developed for contact flocculation-filtration incorporating the flocculation phenomena in ideal conditions. This model was then extended to mobile bed filtration with contact flocculation-filtration arrangement and verified with laboratory-scale mobile bed filter experimental results obtained.

Modelling

Contact flocculation filtration

O'Melia-Alis' model for deep bed filtration was modified for contact-flocculation filtration with the following assumptions.

It is assumed that no floc formation takes place before the suspension-flocculant mixture reaches the filter bed.

When this flocculant-suspension mixture passes through the proes of the filter bed, the headloss is developed which results in a velocity gradient within the filter bed. Due to this velocity gradient, particles aggregate in the form of flocs within the filter bed.

This change in velocity gradient due to headloss development leads to the floc growth and facilitates the retention of particles in the filter medium.

All flocs are spherical in shape.

At a particular filtration time (t) and at a fixed filter depth interval (ΔL) all the flocs have same diameter. *ie* $df(L,t) =$ constant.

The single collector removal efficiency (η_r) for deep bed filtration is defined[5] as:

$$\eta_R = \frac{\text{Rate at which particles } \ddot{N}x \text{ strike and attach the filter grain + Rate at which particles strike and attach a particle collector}}{\text{Rate at which particles flow towards the collector}} \quad (1)$$

Where N is the number of retained particles acting as a collector.

But, in the case of contact-flocculation filtration process, the particles will be present in the form of flocs, as the flocculation occurs within the filter bed. Therefore the expression for η_r has to be modified. Table I illustrates the pattern of change in diameter and number of flocs with time.

The calculation of floc diameter requires an experimental investigation with laboratory-scale flocculation unit with the same raw water to be treated and it is discussed later.

If one assumes, a size distribution of flocs as given in Table I, then the equation for (η_R) will be modified as:

TABLE I: Floc growth profile at a given filter depth

Time	Floc diameter *(df)*	No of floc
o	$dF(L,O)$	$N_o(L,O)$
$o - \Delta t$	$dF(L,\Delta t)$	$N_1(L,\Delta t)$
$\Delta t - 2\Delta t$	$dF(L,2\Delta t)$	$N_2(L,2\Delta t)$
$2\Delta t - 3\Delta t$	$dF(L,3\Delta t)$	$N_3(L,3\Delta t)$
—	—	—
$(n-1)\Delta t - n(\Delta t)$	$dF(L,t)$	$N_n(L,t)$

$$\eta_R(L,t) = \frac{\alpha \cdot \eta \cdot (\pi/4) \cdot dC^2 \cdot V \cdot n_F \cdot (L,t) + \alpha_F \cdot \eta_F \cdot (\pi/4) \cdot V \cdot n_F(L,t) \begin{bmatrix} N_o(L,0) \cdot \{d_F(L,0)\}^2 + \\ N_1(L,\Delta t) \cdot \{d_F(L,\Delta t)\}^2 + \\ \cdots\cdots\cdots\cdots \\ N_n(L,t) \cdot \{d_F(L,t)\}^2 \end{bmatrix}}{\left[\frac{\pi}{4}\right] \cdot d_c^2 \cdot V \cdot n_F(L,t)} \qquad (2)$$

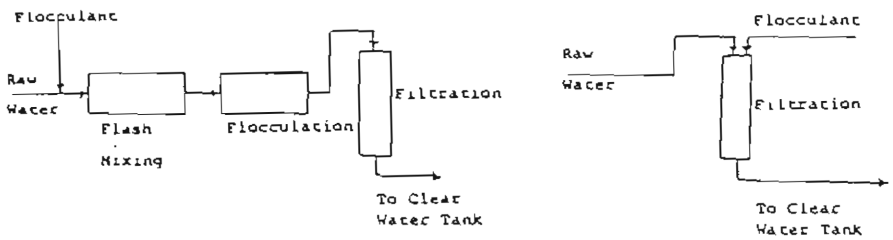

Figure 1: Direct filtration and contact-flocculation filtration process

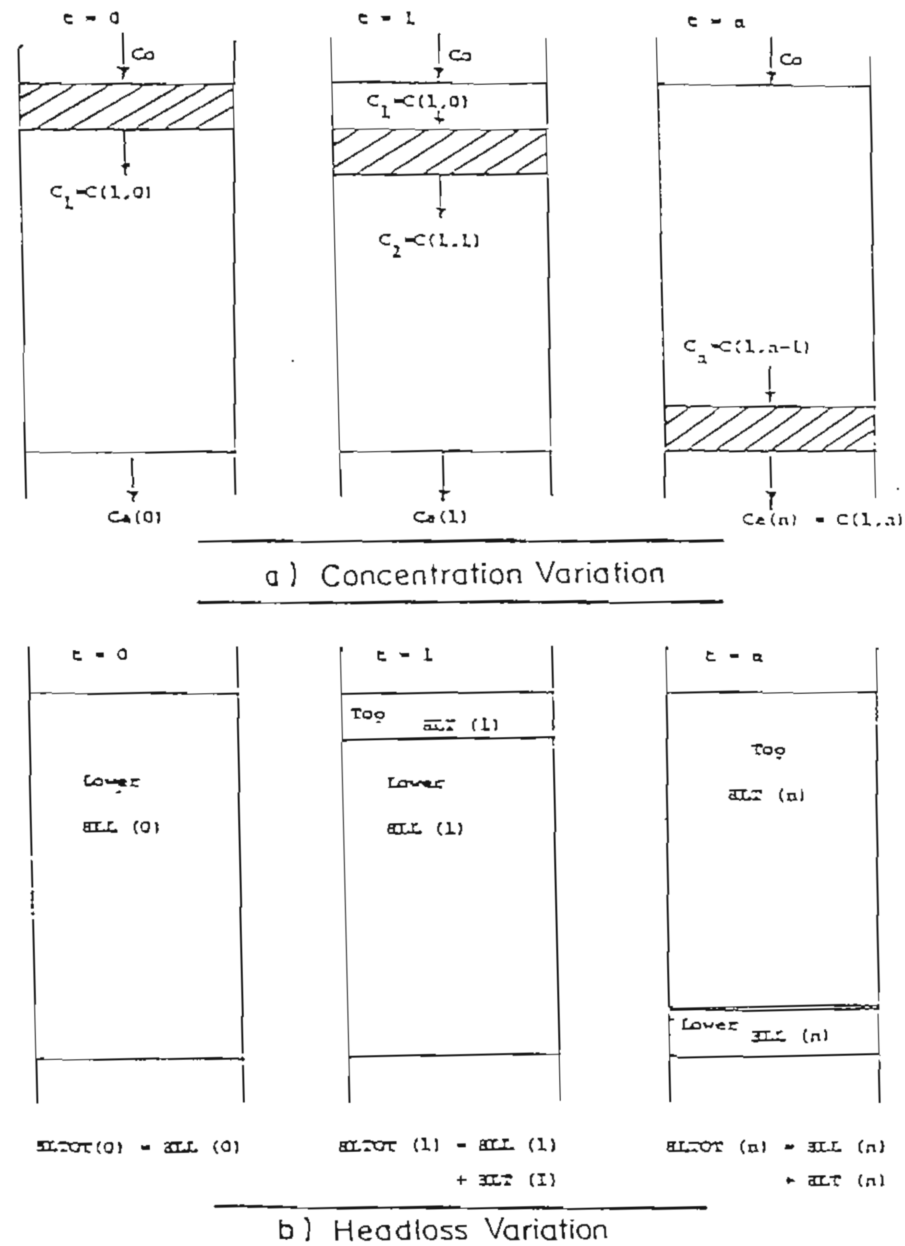

Figure 2: The sand layer movement pattern

Rearrangement of the above equation yields:

$$\eta_R(L,t) = \alpha\eta + \frac{\alpha_F \cdot \eta_F}{d_c^2} \left[\sum_{i=0}^{n=t} N_i(L,t_i)\{d_F(L,t_i)\}^2 \right] \qquad (3)$$

Where η, η_F are the contact efficiencies of a filter grain and floc (particle) collector

α, α_F are the attachment coefficients, between filter grain to floc and floc to floc

d_F, d_c are the diameters of flocs and filter grain

$N(L,t)$ is the number of particle collector at depth interval (L to L+Δ) L and time (t)

$nF(L,t)$ is the floc number concentration at depth L and time t.

In the Equation 3 the first term on the R.H.S. represents the removal efficiency of a single filter grain and the second term represents the increase in the removal brought by the flocs attached to the filter grain.

The change of number of particle collectors with time can be calculated from the following[5] equation.

$$\frac{d\, N(L,t)}{dt} = \alpha\eta \cdot \beta \cdot V \cdot n_F(L,t) \cdot (\pi/4) \cdot d_c^2 \qquad (4)$$

where ß is the fraction of retained flocs acting as particle collectors.

The number of particle collectors at a given time can be calculated from the following equation which is a partial differential form of the above equation.

$$N(L,t) = N(L,t-\Delta t) + \{n_F(L,t-\Delta t) - n_F(L,t)\} \cdot V \cdot A \cdot \Delta t \qquad (5)$$

From the mass balance of suspended particles removal the following equation can be obtained:

$$\frac{d\, n_F(L,t)}{dt} + V \cdot \frac{d\, n_F(L,t)}{dL} + \left(\frac{3}{2}\right) \eta_R(L,t) \cdot V \cdot n_F(L,t) \cdot \frac{(1-f)}{.dC} = 0 \qquad (6)$$

η_R and $\eta_F(L,t)$ at different depths and time can be calculated by solving the Equations 3 through 6. Since there is no analytical solution, in this study, these equations were solved considering η_R and $\eta_F(L,t)$ as step function of time as have been treated by O'Melia and Ali[5]. The final equation obtained for η_R (at depth L and time t) is as follows:

$$\eta_R(L,t) = \alpha\eta\left[1 + \eta_F \cdot \alpha_F \cdot \beta \cdot V \cdot \left(\frac{\pi}{4}\right) \cdot \sum_{i=0}^{n=t}\left[\exp \cdot \left\{-\left(\frac{3}{2}\right) \cdot (1-f) \cdot \eta_R(L,t_{i-1}) \cdot \frac{\Delta L}{d_c}\right\} \cdot \Delta t \cdot \eta_F(L,t_{i-1}) \cdot d_F(L,t_i)\right]^2\right] \quad (7)$$

Kozeny's equation for the calculation of clean bed headloss development is:

$$\frac{h_{fo}}{L} = K \cdot \frac{\mu}{\rho_\ell} \cdot \frac{V}{g} \cdot \frac{(1-f)^2}{f^3} \cdot ag^2 \quad (8)$$

As the filtration proceeds, the specific surface (a_g) is modified due to the deposition of flocs on the filter grains. The change of specific surface can be calculated in the following manner:

$$ag = \frac{A_C + A_F}{V_C + V_F} \quad (9)$$

For the size distribution of flocs given in the Table I, the change in specific surface can be written as follows:

$$ag^2 = \left(\frac{36}{d_c^2}\right) \left[\frac{1 + \beta'(1/N_c \cdot d_c^2) \cdot \sum_{i=0}^{n=t} N_i(L,t_i) \cdot \{d_F(L,t_i)\}^2}{1 + \beta'(1/N_c \cdot d_c^3) \cdot \sum_{i=0}^{n=t} N_i(L,t_i) \cdot \{d_F(L,t_i)\}^2}\right] \quad (10)$$

Where, ß' is the fraction of the total number of retained flocs, that contribute to the additional surface.

Substituting the above value of (a_g^2) in Equation 9, the following equation for headloss can be obtained.

$$\frac{hf(L,t)}{L(t)} = 36 \cdot K \cdot \frac{\mu}{\rho_\ell} \cdot \frac{V}{g} \cdot \frac{(1-f)^2}{f^3} \cdot \frac{1}{d_c^2} \cdot \left[\frac{1 + \beta(1/N_c \cdot d_c^2) \cdot \sum_{i=0}^{n=t} N_i(L,t_i) \cdot [d_F(L,t_i)]^2}{1 + \beta(1/N_c \cdot d_c^3) \cdot \sum_{i=0}^{n=t} N_i(L,t_i) \cdot [d_F(L,t_i)]^2}\right]^2 \quad (11)$$

There exists no general relationship between floc size, velocity gradient and concentration of suspended solids. Therefore in the present study, the semi emperical equations (12) and (13) obtained from Jar Test experiments[6] for the kaolin clay suspension in the presence of Cat Floc-T were used to calculate the ultimate diameter of floc, and floc diameter at different time and depth of the filter.

$$Du = \left[\frac{2238721.01}{\bar{G}}\right]^{0.4} \quad (12)$$

where, G is in sec.
du is in μ m

The floc diameter at different depths and time is given as:

$$d_F(L,t) = \frac{Du \left[\log \frac{d_o}{1 - \frac{d_o}{Du}} + 0.001636 \cdot \bar{G} \cdot t_F\right]}{Du + \left[\log \frac{d_o}{1 - \frac{d_o}{Du}} + 0.001636 \cdot \bar{G} \cdot t_F\right]} \quad (13)$$

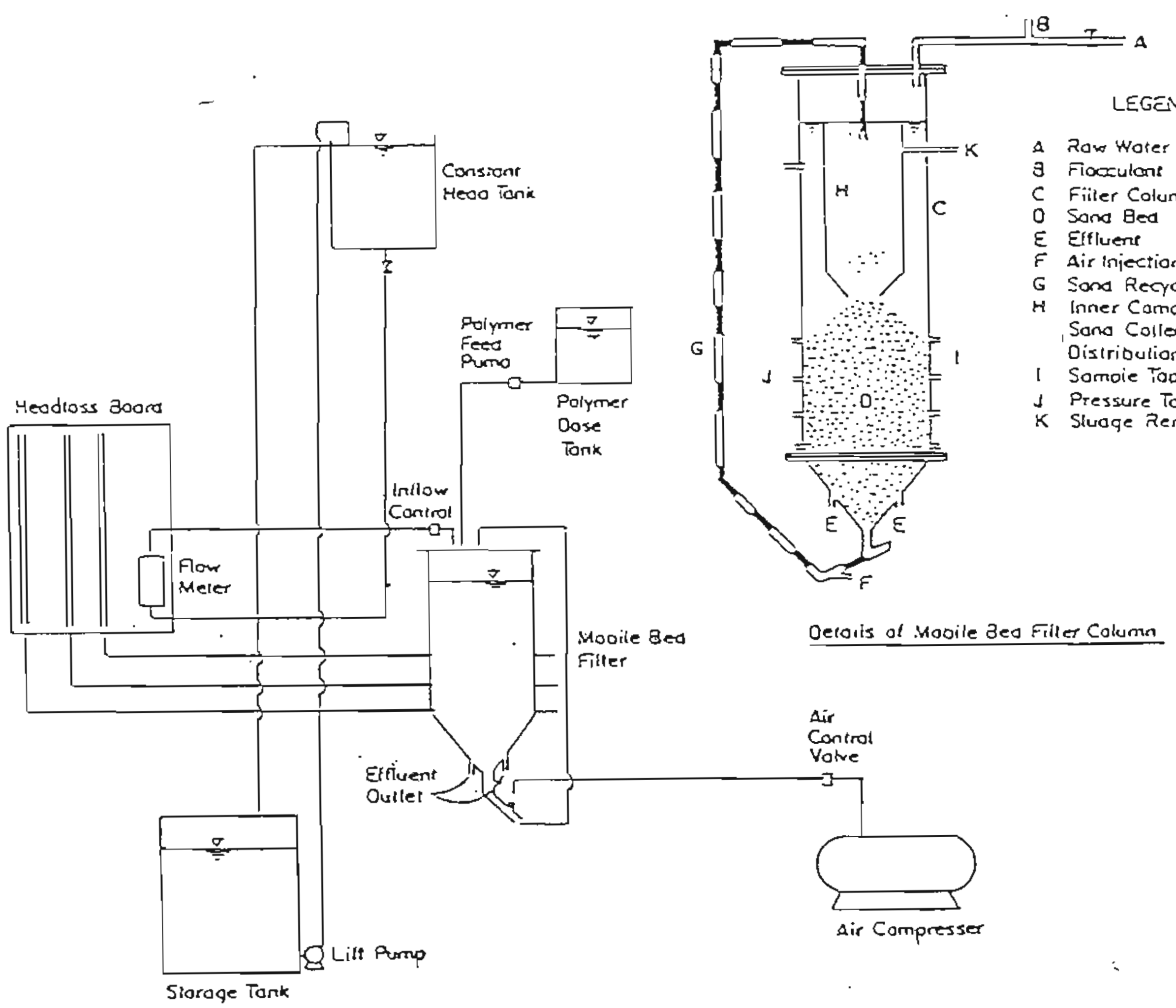

The different steps involved in the proces of floc diameter calculations are summarized here.

Calculation of velocity gradient ($\bar{G}$): The velocity gradient ($\bar{G}$) was calculated from the following relationship:

$$\bar{G} = P/\mu V \tag{14}$$

Where P is the power dissipated within the filter layer which can be calculated from the following relationship:

$$P = \left[\Delta H(L+\Delta L, t+\Delta t) - \Delta H(L, t+\Delta t)\right]Q\rho g \tag{15}$$

Where V is the filter bed volume of the layer considered

Q is the flow rate of the suspension

Calculation of ultimate floc diameter: The ultimate floc diameter was calculated using the G values calculated and Equation 12 at different depths and time.

Calculation of floc diameter: The floc diameter at different depths and time was then computed using Equation 13. It should be noted that the formulation of Equation 13 was based on Boadway's approach.[7]

Mobile bed with contact flocculation-filtration

The developed model for fixed bed filters with contact-flocculation filtration arrangement was modified to mobile bed filters considering the relative approach velocity of suspension with respect to sand layer movement (Vr). The calculation process is briefly schematized in Figure 2. The final equations for single collector removal efficiency and headloss in the mobile bed filter are as presented below:

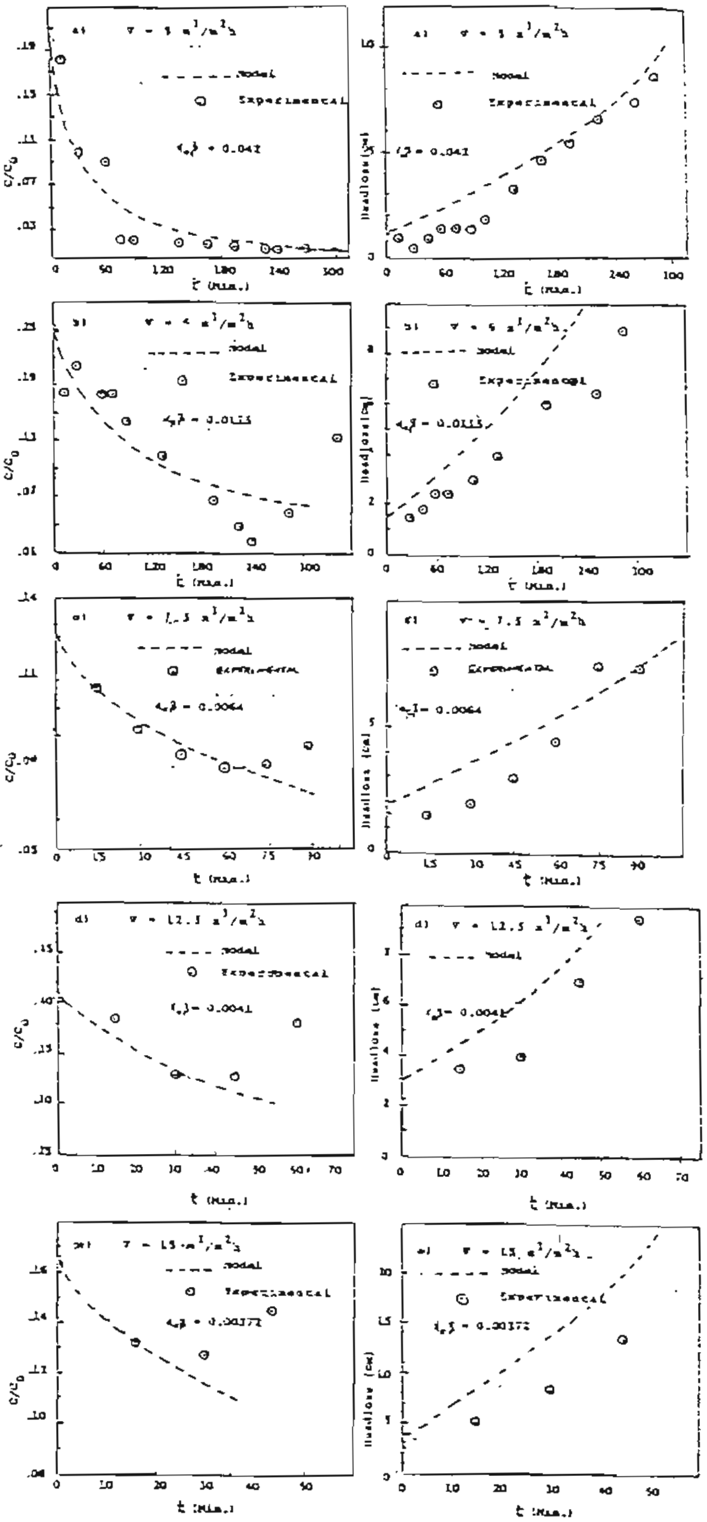

Figure 4: Experimental and theoretical concentration and headloss profiles *(Media size = 0.10045 cm; Polymer dose = 0.05 mg/l)*

$$\eta_R(L,t) = \alpha\eta\cdot\Big[1 + \eta_F\cdot\alpha_F\cdot\beta\cdot (V-V_r)\cdot\left(\frac{t}{4}\right)\sum_{i=0}^{n=t}\left[\exp\left(-\left(\frac{3}{2}\right)\cdot(1-f)\cdot\eta_R(L,t_{i-1})\right)\right]\cdot\frac{\Delta L}{d_c}\cdot\Delta t\cdot\eta_F(L,t_{i-1})\cdot\left[d_F(L,t_i)\right]^2\Big] \tag{16}$$

$$\frac{h_f(L,t)}{L(t)} = 36\cdot K\cdot\frac{\mu}{\rho_\ell}\cdot\frac{(V-V_r)}{g}\cdot\frac{(1-f)^2}{f^3}\cdot\frac{t}{d_c^2}\left[\frac{1+\beta'(1/N_c d_c^2)\cdot\sum_{i=0}^{n=t}N_i(L,t_i)\cdot d_F(L,t_i)^2}{1+\beta'(1/N_c d_c^3)\cdot\sum_{i=0}^{n=t}N_i(L,t_i)\cdot d_F(L,t_i)^3}\right]^2 \tag{17}$$

Experimental

A set of experiments were carried out with laboratory-scale fixed bed and mobile bed filter models. The mobile bed filter model used in the study is presented in Figure 3.

Sand with sizes ranging from 0.841-1.168mm was selected as the filter

Mobile bed filtration with contact flocculation-filtration arrangement: As in the case of fixed bed filtration model, the clean bed removal efficiency for the mobile bed filtration model, $\alpha_p\beta$ was calculated from the experimental data. Then C/Co profiles at different recycle rate were simulated. It was noticed that the C/Co profiles could not be simulated with the same $\alpha_p\beta$ used for fixed-bed filter experiments (Figure 4). This is the main drawback of the modified model.

Conclusions

The O'Melia-Ali's model can be modified for contact-flocculation filtration by taking into account the flocculation phenomena within the filter bed. This requires the development of empirical equations relating the floc size variation with velocity gradient and flocculation time from laboratory-scale flocculation experiments with the same suspension used for filtration. The value $\alpha_p\beta$ appearing in the model was found to decrease with the increase in filtration velocity instead of remaining constant. This is a short-coming of this model.

The removal efficiency of mobile bed filter (with contact flocculation-filtration arrangement) could not be successfully simulated for different recycle rates from the modified O'Melia and Ali's model incorporating the sand layer movement using the same value of $\alpha_p\beta$ calculated for the fixed bed filter under identical operating conditions. A further modification of the model is therefore essential.

References

1 ALLANSON JT and AUSTIN EP, Development of Continuous Inclined Sand Filter, *Filtration and Separation*, **3**/4, pp 165-169, 1976.

2 ANONYMOUS, The *Simator* Continuous Sand Filter. *Water and Waste Water Engineering*, 72, pp 20-24, 1968.

3 AL ALOUSI, La Filtration dans la masse en epuration tertiaire D'eaux residuaires, unpublished PhD Thesis, Academie de Montpeller, Universitie des Sciences et Techniques du languedoc, France, 1979.

4 TRAITEMENT TERITAIRE, Performance du Filtre a Sable Tenten a Lavage Continue, *Report Agence Financiere de Bassin Scene Normandie*, 1979.

5 O'MELIA CR and ALI W, The Role of Retained Particles in Deep Bed Filtration, *Progress in Water Technology*, **10**, No 5/6, pp. 123-137, 1978.

6 LIANG AN-SHU, Technical Comparison of Direct Filtration and Contact Flocculation-filtration process, *Masters' Thesis, Asian Institute of Technology*, No EV-82-11, 1982.

7 BOADWAY JD, Dynamics of Growth and Breakage of Alum Floc in Presence of Fluid Shear, *Journal of the Environmental Engineering Division, ASCE*, **104**, No EE5, pp 901-915, 1978.

The authors are both in the environmental engineering division of the Asian Institute of Technology in Bangkok, Thailand. ■

Plant & Products

Analogue pH meter

Ideal for environmental applications, *Delta 115* is robustly constructed in Noryl to ensure it can withstand the rigours imposed by inexperienced users, and its battery/mains power option allows complete portability. Over 1000 hours of continuous use are provided by two 9-volt batteries.

A mirror-backed scale aids precise readings between 0-14 pH and over the range ±700mV; control facilities are provided for: pH; mV; calibration; slope; battery check and temperature compensation. There is also the facility for automatic temperature compensation if an additional probe accessory is fitted.

The *Delta 115* is supplied ready for immediate use, complete with: electrode; stand; buffer powders and battery eliminator.

Reader Service No. 1

Sludgepress range

Currently available in 3 belt widths, the Series 3 is a development of the Series 2 with increased drainage and pressure zones and is capable of higher sludge loadings with reduced moisture content in the final discharged cake.

Ideally suited for dewatering anaerobic digested sludges, 5 - Series 3 units are in operation in Philadelphia, USA and are achieving a dewatering rate of 600 kgs solids per metre belt width per hour, with the feed containing 3-4% solids W/W and final cake, 30% solids W/W.

To compliment the Series 3 Sludgepress range, a pre-thickener is also available. Mounted above the main press unit, the pre-thickener will accept the thin sludges and increase the solids content by gravity drainage, so reducing the hydraulic loading on the main press and enabling it to operate at optimum conditions.

Reader Service No. 2

Coating material

A new low-bake Duraguard P3353 series of electrostatic polyester powder paints is launched which it is claimed can shorten the process time by 20% and reduce energy consumption by up to 10% over standard polyester and other electrostatic powder, whilst retaining full physical properties.

Other features include:

Extensive new colour range of 30 RAL colours, high abrasion and chip resistance, typical cure schedule of eight minutes at 180°C, single coat application from 40 to 150 microns and suitable for use with existing electrostatic equipment.

Reader Service No. 3

New brochure

Rosemount's highly successful Series 4000 and 4001 alarm monitors have been used in a very wide variety of applications, many of which have been innovative.

This new brochure focusses on six representative examples developed from actual field experience. They illustrate how the special features of the alarm monitor can be used in measurement, monitoring and control applications of every sort.

Included are the temperature monitoring of rotating machines, pump performance monitoring, the monitoring and control of processes, process machinery monitoring, pump switching and cyclical pumping control.

Reader Service No. 4

Continued on page 330